

## Synthesis, molecular structure and biological activity of Ni<sup>II</sup> complexes based on substituted 2-(2-hydroxyphenyl)benzoxazole

Inna O. Tupaeva,<sup>\*a</sup> Oleg P. Demidov,<sup>b</sup> Elena V. Vetrova,<sup>a</sup> Evgeniy A. Gusakov,<sup>a</sup> Tatyana A. Krasnikova,<sup>a</sup> Leonid D. Popov,<sup>c</sup> Alexander A. Zubenko,<sup>d</sup> Leonid N. Fetisov,<sup>d</sup> Yurii A. Sayapin,<sup>e</sup> Anatoly V. Metelitsa<sup>a</sup> and Vladimir I. Minkin<sup>a</sup>

<sup>a</sup> Institute of Physical and Organic Chemistry, Southern Federal University, 344090 Rostov-on-Don, Russian Federation. E-mail: iotupaeva@sfnu.ru

<sup>b</sup> North-Caucasus Federal University, 355009 Stavropol, Russian Federation

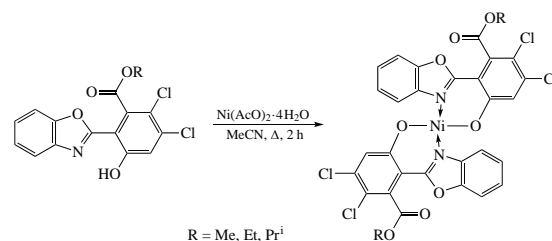
<sup>c</sup> Department of Chemistry, Southern Federal University, 344090 Rostov-on-Don, Russian Federation

<sup>d</sup> North-Caucasian Zonal Research Veterinary Institute, 346406 Novocherkassk, Russian Federation

<sup>e</sup> Southern Scientific Centre of the Russian Academy of Sciences, 344006 Rostov-on-Don, Russian Federation

DOI: 10.1016/j.mencom.2022.11.018

New Ni<sup>II</sup> complexes based on the substituted 2-(2-hydroxyphenyl)benzoxazole have been synthesized from the corresponding ligands and nickel acetate. The crystal structure of bis[2-(1,3-benzoxazol-2-yl-κN)-4,5-dichloro-3-(methoxycarbonyl)phenolate-κO]nickel(II) has been determined by X-ray diffraction. The new Ni<sup>II</sup> complexes have been screened for their antibacterial, protistocidal and fungistatic activities.



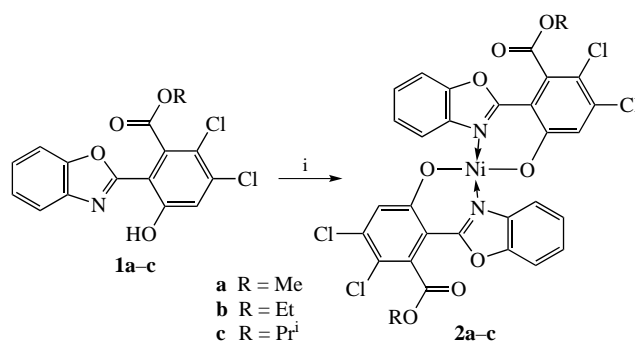
**Keywords:** 2-(2-hydroxyphenyl)benzoxazole, nickel(II) complexes, X-ray diffraction analysis, antibacterial activity.

Molecular systems based on benzoxazoles and their derivatives, e.g. 2-(2-hydroxyphenyl)benzoxazoles, exhibit antimicrobial,<sup>1–4</sup> antibacterial,<sup>5–7</sup> antiviral,<sup>8</sup> antifungal,<sup>6,9</sup> anticancer,<sup>8–11</sup> anti-inflammatory<sup>12,13</sup> and antiproliferative<sup>14</sup> activities as well as can serve as HIV-1<sup>15,16</sup> and PDE417 reverse transcriptase inhibitors. Derivatives of 2-(2-hydroxyphenyl)benzoxazoles are strong coordinating agents and would form stable complexes with various transition metals. Zinc(II) complexes based on 2-(2-hydroxyphenyl)benzoxazoles demonstrate nontrivial spectral-luminescent properties and electroluminescence, which allows them to be used as components of active layers of OLED and fluorescent sensors.<sup>18–22</sup> Moreover, complexes of benzoxazole derivatives are promising systems for bio-imaging<sup>23</sup> and therapeutic agents with pronounced biological activity.<sup>24–29</sup> Therefore, search for new coordination systems based on 2-(2-hydroxyphenyl)benzoxazoles is an urgent task.

Recently, we have investigated the chromogenic properties of 2-(6-hydroxy-2-methoxycarbonylphenyl)benzoxazole and have obtained its complexes with Zn<sup>II</sup> and Cd<sup>II</sup> which possessed effective blue fluorescence and resistance to photodegradation.<sup>30</sup> In this work, we synthesized and explored three new Ni<sup>II</sup> complexes based on 2-(2-alkoxycarbonyl-6-hydroxyphenyl)benzoxazoles **1a–c** (Scheme 1). Ligands **1a–c** were previously obtained by contraction of seven-membered ring in 2-benzoxazol-2-yl-5,6,7-trichloro-1,3-tropolone under prolonged heating in the corresponding alcohol (MeOH, EtOH or Pr<sup>i</sup>OH).<sup>31,32</sup> According to the elemental analysis data, the reaction of 2-(alkoxycarbonyl-3,4-dichloro-6-hydroxyphenyl)benzoxazoles (R = Me, Et, Pr<sup>i</sup>) **1a–c** with nickel(II) acetate in acetonitrile in a ligand/metal ratio of 2:1 results in the formation of corresponding mononuclear bis-chelate Ni<sup>II</sup> complexes **2a–c** (see Scheme 1).

<sup>1</sup>H NMR spectra of compounds **2a–c** revealed a significant broadening of the lines (especially the signals of aromatic protons), which may indicate a partial or predominant paramagnetic behaviour of the central atom as well as a non-planar structure of the chelate node of the complexes. In this regard, <sup>1</sup>H NMR spectral data are not informative to confirming the structure of complexes **2a–c** (see Online Supplementary Materials, Figures S1–S3).

IR spectra of ligands **1a–c** reveal the following: a broadened band in the region of 3000–3450 cm<sup>−1</sup> related to the oscillation of the OH group bound by a hydrogen bond, a high-intensity absorbance band of C=O group of the ether fragment in the region of 1731–1737 cm<sup>−1</sup> and absorption bands in the region of ca. 1620 cm<sup>−1</sup> related to stretching vibrations of the azole C=N bond. Disappearance of the absorbance band of the OH group and a shift to the low-frequency region of the valence vibrations of the C=N bond by ~15 cm<sup>−1</sup>, which are observed during



**Scheme 1** Reagents and conditions: i, Ni(AcO)<sub>2</sub>·4H<sub>2</sub>O, MeCN, 70–80 °C, 2 h.

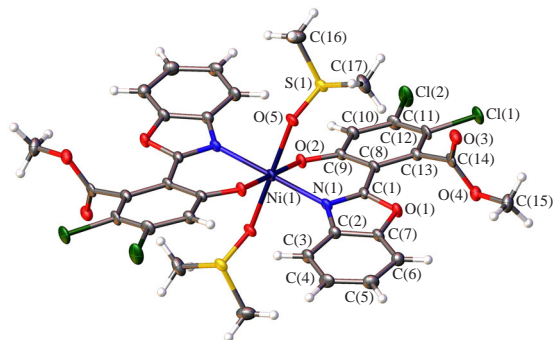


**Figure 1** Molecular structure of complex **2a** containing two DMSO molecules in the representation of atoms by ellipsoids of thermal oscillations with a 50% probability.

complexation, prove the formation of a chelate complex. Complexes **2a–c** are also characterized by the appearance of new bands in the region of  $\sim 545$  and  $\sim 515$   $\text{cm}^{-1}$  caused by fluctuations of  $\nu(\text{Ni–O})$  and  $\nu(\text{Ni–N})$ , respectively (see Online Supplementary Materials, Figures S4–S6).<sup>33</sup>

The structure of bis[2-(1,3-benzoxazol-2-yl- $\kappa\text{N}$ )-4,5-dichloro-3-(methoxycarbonyl)phenolate- $\kappa\text{O}$ ]nickel(II) **2a** complex (Figure 1) was established by X-ray diffraction analysis; the main distances and angles in the molecule are given in Tables S1–S4 and Figure S7 (see Online Supplementary Materials).<sup>†</sup> According to X-ray diffraction data, compound **2a** crystallizes in a centrosymmetric space group ( $P2_1/n$ ) with a nickel ion located in the inversion center. An asymmetric unit consists of half of a complex molecule. The distances and bond angles are within the expected values. The donor atoms N(1), O(2) and O(5) in the composition of the oxazole cycle, phenolic fragment and sulfoxide form slightly distorted octahedral environment around the nickel(II) ion. The octahedron is elongated in vertex positions. The bond distance Ni(1)–N(1) is 2.066(2) Å, while the bond lengths Ni(1)–O(2) and Ni(1)–O(5) are 2.0015(17) and 2.1192(18) Å, respectively. These values, in general, slightly differ from the bond lengths (2.1212, 2.0076 and 2.2140 Å, respectively) in the zinc complex described earlier.<sup>30</sup> The shortest intermolecular contact is detected between the oxazole fragment and the ester oxygen atom [the oxazole plane is O(4) 2.979 Å]. A fragment of the molecular packaging is shown in Figure S8 (Online Supplementary Materials).

The electron absorption spectra of new complexes **2a–c** in DMSO (Figure 2, Table 1) contain a long-wavelength band with a maximum at 393–394 nm and a molar extinction coefficient of 27800–27900  $\text{dm}^3 \text{mol}^{-1} \text{cm}^{-1}$ . These bands are asymmetrical and have a shoulder at 406–407 nm. The short-

<sup>†</sup> Crystal data for **2a**.  $\text{C}_{34}\text{H}_{28}\text{Cl}_4\text{N}_2\text{NiO}_{10}\text{S}_2$  ( $M = 889.21$   $\text{g mol}^{-1}$ ), monoclinic, space group  $P2_1/n$  (no. 14),  $a = 10.6083(2)$ ,  $b = 7.8650(2)$  and  $c = 21.3907(4)$  Å,  $\beta = 95.427(2)^\circ$ ,  $V = 1776.72(7)$  Å<sup>3</sup>,  $Z = 2$ ,  $\mu(\text{CuK}\alpha) = 5.192$   $\text{mm}^{-1}$ ,  $T = 99.98(18)$  K,  $d_{\text{calc}} = 1.662$   $\text{g cm}^{-3}$ , 18293 reflections measured ( $8.304^\circ \leq 2\theta \leq 152.668^\circ$ ), 3681 unique ( $R_{\text{int}} = 0.0680$ ,  $R_{\text{sigma}} = 0.0408$ ) which were used in all calculations. The final  $R_1$  was 0.0474 [ $I > 2\sigma(I)$ ] and  $wR_2$  was 0.1294 (all data). The experimental data for structure **2a** were obtained on an Agilent SuperNova diffractometer using a microfocus X-ray source with copper anode and an Atlas S2 two-dimensional CCD detector. The reflections were collected, unit cell parameters determined and refined using the specialized CrysAlisPro 1.171.38.41 software suite (Rigaku Oxford Diffraction, 2015).<sup>34</sup> The structures were solved using the ShelXT program (Sheldrick, 2015)<sup>35</sup> and refined with the ShelXL program (Sheldrick, 2015).<sup>36</sup> Molecular graphics and presentation of structures for publication were performed with the Olex<sup>2</sup> v1.5 software suite.<sup>37</sup>

CCDC 2166674 contains the supplementary crystallographic data for this paper. These data can be obtained free of charge from The Cambridge Crystallographic Data Centre via <http://www.ccdc.cam.ac.uk>.

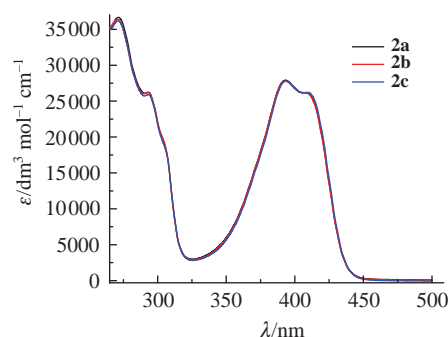


**Figure 2** Electron absorption spectra of nickel complexes **2a–c** in DMSO.

**Table 1** UV-VIS data of complexes **2a–c** in DMSO.

Compound	$\lambda_{\text{max}}$ (nm)/ $\epsilon$ ( $10^3 \text{ dm}^3 \text{ mol}^{-1} \text{ cm}^{-1}$ )
<b>2a</b>	393 (27.9), 406 <sup>sh</sup> (26.2), 293 <sup>sh</sup> (26.0), 271 (36.3)
<b>2b</b>	394 (27.8), 407 <sup>sh</sup> (26.2), 293 <sup>sh</sup> (26.3), 270 (36.4)
<b>2c</b>	393 (27.9), 406 <sup>sh</sup> (26.2), 293 <sup>sh</sup> (26.3), 272 (36.7)

wave absorption band is localized at 270–272 nm with a molar extinction coefficient of 36300–36700  $\text{dm}^3 \text{mol}^{-1} \text{cm}^{-1}$ . Detailed spectral characteristics of nickel complexes **2a–c** are given in Table 1.

The absorption spectra of complexes **2a–c** are bathochromically shifted (the displacement of the long-wavelength absorption band reaches 43–46 nm) relative to the electron absorption of the corresponding ligands **1a–c**.<sup>30</sup> Significant changes in the electron absorption of the ligands are caused by the interaction of the coordination-active chelate node of 2-(hydroxyphenyl)benzoxazoles with Ni<sup>II</sup> ions and the formation of chelate complexes. These results of the studies showed that the nature of the alkoxy carbonyl substituent in the phenyl fragment of the ligands does not significantly affect the spectral characteristics of the electron absorption of their bis-chelate nickel complexes.

Unlike zinc and cadmium mononuclear bis-chelate complexes<sup>30</sup> possessing intense photoluminescence in the blue region of the spectrum, no fluorescence was detected for nickel analogues **2a–c**. The effect of the nature of the metal is manifested in the longer wavelength absorption of nickel complexes compared to zinc complexes.<sup>29</sup>

The obtained derivatives of 2-(2-hydroxyphenyl)benzoxazoles **1a–c** and their Ni<sup>II</sup> complexes **2a–c** were tested for fungistatic, protistocidal and antibacterial activity (Table 2).

Hence, it was revealed that ligands **1a–c** and their complexes **2a–c** did not possess fungistatic activity against *Penicillium italicum*. The protistocidal activity of compound **1c** against *Colpoda steinii* is 500  $\mu\text{g ml}^{-1}$  that is significantly lower than the activity of the comparison samples; the remaining compounds were inactive. Results of the assessment of antibacterial activity of the compounds **1b,c** and **2b** toward *St. aureus* showed that their activity is 26% of the level of ciprofloxacin activity and 35% of furazolidone activity. For complex **2b**, culture growth retardation zone against *E. coli* was 7–8 mm which corresponded to 38% of the activity of ciprofloxacin and to 33% in comparison with furazolidone.

Thus, ligand 2-(3,4-dichloro-2-ethoxycarbonyl-6-hydroxyphenyl)benzoxazole **1b** and its Ni<sup>II</sup> complex **2b** possessed an average antibacterial activity against gram-positive and gram-negative bacteria *St. aureus*. Complexation of Ni<sup>II</sup> ions with ligand **1b**, which is ineffective against *E. coli*, contributed to the emergence of antibacterial activity of Ni<sup>II</sup> complex **2b** toward gram-positive and gram-negative *E. coli* bacteria.

**Table 2** Fungistatic, protistocidal and antibacterial activity of substituted 2-(2-hydroxyphenyl)benzoxazoles **1a–c** and their Ni<sup>II</sup> complexes **2a–c**.<sup>a</sup>

Compound	Fungistatic activity, growth retardation zone of <i>Penicillium italicum</i> /mm	Protistocidal activity against <i>Colpoda steinii</i> /μg ml <sup>-1</sup>	Bacteriostatic activity, growth retardation zone/mm			
			<i>St. aureus</i>		<i>E. coli</i>	
			+/-	+	+/-	+
<b>1a</b>	0	>500	7	0	7	0
<b>1b</b>	0	>500	0	7	7	0
<b>1c</b>	0	500	0	7	7	0
<b>2a</b>	0	>500	7	0	7	0
<b>2b</b>	0	>500	0	7	0	8
<b>2c</b>	0	>500	7	0	7	0
Fundazol	37±0.03	–		–		–
Ciprofloxacin	–	–		27±0.24		21±0.20
Furazolidone	–	–		20±0.18		24±0.17
Chloroquine	–	15.6±0.14		–		–
Baycox (Toltrazuril)	–	62.5±0.58		–		–

<sup>a</sup>+/- denotes growth retardation noted during the first 12 h, + denotes growth retardation noted for more than 24 h (presumably due to the bactericidal activity).

This research was supported by the Russian Science Foundation no. 21-73-00079, <https://rscf.ru/en/project/21-73-00079/>, at the Southern Federal University.

#### Online Supplementary Materials

Supplementary data associated with this article can be found in the online version at doi: 10.1016/j.mencom.2022.11.018.

#### References

- V. R. Mishra, C. W. Ghanavatkar, S. N. Mali, S. I. Qureshi, H. K. Chaudhari and N. Sekar, *Comput. Biol. Chem.*, 2019, **78**, 330.
- V. S. Padalkar, B. N. Borse, V. D. Gupta, K. R. Phatangare, V. S. Patil, P. G. Umape and N. Sekar, *Arab. J. Chem.*, 2016, **9**, 1125.
- O. Temiz-Arpaci, C. T. Zeyrek, M. Arisoy, M. Erol, I. Celik and F. Kaynak-Onurdag, *J. Mol. Struct.*, 2021, **1245**, 131084.
- N. A. Galieva, D. A. Saveliev, O. S. Eltsov, V. A. Bakulev, G. Lubec, J. Xing, Z. Fan and T. V. Beryozkina, *Mendelev Commun.*, 2021, **31**, 495.
- S. Alper-Hayta, M. Arisoy, O. Temiz-Arpaci, I. Yildiz, E. Aki, S. Ozkan and F. Kaynak, *Eur. J. Med. Chem.*, 2008, **43**, 2568.
- T. Ertan, I. Yildiz, B. Tekiner-Gulbas, K. Bolelli, O. Temiz-Arpaci, S. Ozkan, F. Kaynak, I. Yalcin and E. Aki, *Eur. J. Med. Chem.*, 2009, **44**, 501.
- M. Taşci, O. Terniz-Arpaci, F. Kaynak-Onurdag and S. Okten, *Indian J. Chem., Sect. B: Org. Chem. Incl. Med. Chem.*, 2018, **57**, 385.
- S. M. Rida, F. A. Ashour, S. El-Hawash, M. El-Semary, M. H. Badr and M. A. Shalaby, *Eur. J. Med. Chem.*, 2005, **40**, 949.
- P. K. Jauhari, A. Bhavani, S. Varalwar, K. Singhal and P. Raj, *Med. Chem. Res.*, 2008, **17**, 412.
- D. Kumar, M. R. Jacob, M. B. Reynolds and S. M. Kerwin, *Bioorg. Med. Chem.*, 2002, **10**, 3997.
- M. S. R. Murty, K. R. Ram, R. V. Rao, J. S. Yadav, J. V. Rao, V. T. Cheriyan and R. J. Anto, *Med. Chem. Res.*, 2011, **20**, 576.
- D. Kim, H. Y. Won, E. S. Hwang, Y.-K. Kim and H.-Y. Park Choo, *Bioorg. Med. Chem.*, 2017, **25**, 3127.
- J. Q. Dong, J. Liu and P. C. Smith, *Biochem. Pharmacol.*, 2005, **70**, 937.
- M. A. Abdelgawad, R. B. Bakr and H. A. Omar, *Bioorg. Chem.*, 2017, **74**, 82.
- Ö. Temiz-Arpaci, A. Özdemir, İ. Yalçın, İ. Yıldız, E. Akı-Şener and N. Altanlar, *Arch. Pharm.*, 2005, **338**, 105.
- B.-L. Deng, M. D. Cullen, Z. Zhou, T. L. Hartman, R. W. Buckheit, Jr., C. Pannecouque, E. De Clercq, P. E. Fanwick and M. Cushman, *Bioorg. Med. Chem.*, 2006, **14**, 2366.
- K. Kuroda, S. Tsuyumine and T. Kodama, *Org. Process Res. Dev.*, 2016, **20**, 1053.
- F. Dumur, *Synth. Met.*, 2014, **195**, 241.
- H. Tanaka, S. Tokito, Y. Taga and A. Okada, *J. Mater. Chem.*, 1998, **8**, 1999.
- T. Yasuda, Y. Yamaguchi, K. Fujita and T. Tsutsui, *Chem. Lett.*, 2003, **32**, 644.
- A. Kumar, A. K. Palai, R. Srivastava, P. S. Kadyan, M. N. Kamalasanan and I. Singh, *J. Organomet. Chem.*, 2014, **756**, 38.
- W. S. Kim, J. M. You, B.-J. Lee, Y.-K. Jang, D.-E. Kim and Y.-S. Kwon, *Thin Solid Films*, 2007, **515**, 5070.
- G. Zhang, Y. Zhao, B. Peng, Z. Li, C. Xu, Y. Liu, C. Zhang, N. H. Voelcker, L. Li and W. Huang, *J. Mater. Chem. B*, 2019, **7**, 2252.
- J. Jiang, X. Tang, W. Dou, H. Zhang, W. Liu, C. Wang and J. Zheng, *J. Inorg. Biochem.*, 2010, **104**, 583.
- A. Bouchoucha, A. Terbouche, A. Bourouina and S. Djebbar, *Inorg. Chim. Acta*, 2014, **418**, 187.
- M. K. Samota and G. Seth, *Heteroat. Chem.*, 2010, **21**, 44.
- G. Watanabe, H. Sekiya, E. Tamai, R. Saijo, H. Uno, S. Mori, T. Tanaka, J. Maki and M. Kawase, *Chem. Pharm. Bull.*, 2018, **66**, 732.
- G. Spengler, A. Kincses, B. Rácz, B. Varga, G. Watanabe, R. Saijo, H. Sekiya, E. Tamai, J. Maki, J. Molnár and M. Kawase, *Anticancer Res.*, 2018, **38**, 6181.
- A. Kincses, S. Szabó, B. Rácz, N. Szemerédi, G. Watanabe, R. Saijo, H. Sekiya, E. Tamai, J. Molnár, M. Kawase and G. Spengler, *Antibiotics*, 2020, **9**, 649.
- E. V. Vetrova, I. O. Tupaeva, Y. A. Sayapin, E. A. Gusakov, S. A. Nikolaevskii, O. P. Demidov, V. I. Minkin and A. V. Metelitsa, *Dyes Pigm.*, 2020, **180**, 108417.
- Y. A. Sayapin, I. O. Tupaeva, A. A. Kolodina, E. A. Gusakov, V. N. Komissarov, I. V. Dorogan, N. I. Makarova, A. V. Metelitsa, V. V. Tkachev, S. M. Aldoshin and V. I. Minkin, *Beilstein J. Org. Chem.*, 2015, **11**, 2179.
- I. O. Tupaeva, Yu. A. Sayapin, Z. N. Bang, V. N. Komissarov, V. V. Tkachev, G. V. Shilov, S. M. Aldoshin and V. I. Minkin, *Russ. Chem. Bull.*, 2013, **62**, 492 (*Izv. Akad. Nauk, Ser. Khim.*, 2013, 491).
- S. Layek, B. Agrahari, A. Kumar, N. Dege and D. D. Pathak, *Inorg. Chim. Acta*, 2020, **500**, 119222.
- CrysAlisPro, version 1.171.38.41*, Rigaku Oxford Diffraction, 2015, <https://www.rigaku.com/en/products/smc/crystalis>.
- G. M. Sheldrick, *Acta Crystallogr., Sect. A: Found. Adv.*, 2015, **71**, 3.
- G. M. Sheldrick, *Acta Crystallogr., Sect. C: Struct. Chem.*, 2015, **71**, 3.
- O. V. Dolomanov, L. J. Bourhis, R. J. Gildea, J. A. K. Howard and H. Puschmann, *J. Appl. Crystallogr.*, 2009, **42**, 339.

Received: 27th April 2022; Com. 22/6885